university of groningen

University Medical Center Groningen

University of Groningen

Atomically Thin Mica Flakes and Their Application as Ultrathin Insulating Substrates for Graphene

Castellanos-Gomez, Andres; Wojtaszek, Magdalena; Tombros, Nikolaos; Agrait, Nicolas; van Wees, Bart; Rubio-Bollinger, Gabino; Agraït, Nicolás

Published in:
Small

DOI:
10.1002/smll.201100733

IMPORTANT NOTE: You are advised to consult the publisher's version (publisher's PDF) if you wish to cite from it. Please check the document version below.

Document Version
Publisher's PDF, also known as Version of record

Publication date:
2011

Link to publication in University of Groningen/UMCG research database

Citation for published version (APA):
Castellanos-Gomez, A., Wojtaszek, M., Tombros, N., Agrait, N., van Wees, B. J., Rubio-Bollinger, G., & Agraït, N. (2011). Atomically Thin Mica Flakes and Their Application as Ultrathin Insulating Substrates for Graphene. Small, 7(17), 2491-2497. DOI: 10.1002/smll.201100733

Copyright
Other than for strictly personal use, it is not permitted to download or to forward/distribute the text or part of it without the consent of the author(s) and/or copyright holder(s), unless the work is under an open content license (like Creative Commons).

Take-down policy
If you believe that this document breaches copyright please contact us providing details, and we will remove access to the work immediately and investigate your claim.

Downloaded from the University of Groningen/UMCG research database (Pure): http://www.rug.nl/research/portal. For technical reasons the number of authors shown on this cover page is limited to 10 maximum.

Download date: 10-02-2018

Atomically Thin Mica Flakes and Their Application as Ultrathin Insulating Substrates for Graphene

Andres Castellanos-Gomez, Magdalena Wojtaszek, Nikolaos Tombros, Nicolás Agraït, Bart J. van Wees, and Gabino Rubio-Bollinger**

***B**y mechanical exfoliation, it is possible to deposit atomically thin mica flakes down to single-monolayer thickness on SiO_2/Si wafers. The optical contrast of these mica flakes on top of a SiO_2/Si substrate depends on their thickness, the illumination wavelength, and the SiO_2 substrate thickness, and can be quantitatively accounted for by a Fresnel-law-based model. The preparation of atomically thin insulating crystalline sheets will enable the fabrication of ultrathin, defect-free insulating substrates, dielectric barriers, or planar electron-tunneling junctions. Additionally, it is shown that few-layer graphene flakes can be deposited on top of a previously transferred mica flake. Our transfer method relies on viscoelastic stamps, as used for soft lithography. A Raman spectroscopy study shows that such an all-dry deposition technique yields cleaner and higher-quality flakes than conventional wet-transfer procedures based on lithographic resists.*

Dr. A. Castellanos-Gomez,[+] Prof. N. Agraït,
Prof. G. Rubio-Bollinger
Departamento de Física de la Materia Condensada
Universidad Autónoma de Madrid
Campus de Cantoblanco, E-28049 Madrid, Spain
E-mail: a.castellanosgomez@tudelft.nl; gabino.rubio@uam.es

Dr. A. Castellanos-Gomez,[+] M. Wojtaszek, Dr. N. Tombros,
Prof. B. J. van Wees
Physics of Nanodevices, Zernike Institute for Advanced Materials
University of Groningen, The Netherlands

Dr. N. Tombros
Molecular Electronics
Zernike Institute for Advanced Materials
University of Groningen, The Netherlands

Prof. N. Agraït, Prof. G. Rubio-Bollinger
Instituto Universitario de Ciencia de Materiales "Nicolás Cabrera"
Universidad Autónoma de Madrid
Campus de Cantoblanco, E-28049 Madrid, Spain

Prof. N. Agraït
Instituto Madrileño de Estudios Avanzados en Nanociencia
IMDEA-Nanociencia, E-28049 Madrid, Spain

[+] Current address: Kavli Institute of Nanoscience, Delft University of Technology, Lorentzweg 1, 2628 CJ Delft, The Netherlands

DOI: 10.1002/smll.201100733

1. Introduction

The experimental realization of graphene, just a single atomic layer of graphite, by mechanical exfoliation of graphite on SiO_2[1,2] surfaces has paved the way to study a very interesting family of 2D crystals almost unexplored so far. Apart from graphene, mechanical exfoliation has been used to prepare other atomically thin crystals[1] such as MoS_2,[3–6] a semiconductor. However, apart from conducting and semiconducting materials, the microelectronic industry also needs insulators that can be used as substrates, dielectrics, or electron-tunnelling barriers. Mechanical exfoliation also enables the production of atomically thin, insulating crystals but, up to now, the fabrication has been restricted to a few insulating 2D crystals such as hexagonal boron nitride.[7,8]

The layered structure of muscovite mica, a phyllosilicate mineral of aluminum and potassium with chemical formula $(KF)_2(Al_2O_3)_3(SiO_2)_6(H_2O)$, makes this material a promising candidate to produce atomically thin insulating crystals by mechanical exfoliation. Moreover, due to its high resistance to heat, water, and chemical agents, its mechanical properties, and to its high dielectric constant, bulk mica has already been

 © 2011 Wiley-VCH Verlag GmbH & Co. KGaA, Weinheim

extensively used in the electronic industry in many applications as a substrate, heat and electrical insulator, or dielectric barrier. Recently, bulk mica has been also employed as a substrate to fabricate ultraflat graphene samples.[9] It has been observed that graphene deposited on mica adheres to the atomically flat terraces of mica without noticeable rippling. Note that the ripples in graphene, unavoidable when it is either deposited on SiO_2[10] or suspended,[11] can modify its electronic properties and induce charge inhomogeneities.[12,13] It would be therefore very interesting to study how the atomically flat topography of graphene on mica affects the electronic properties of graphene. The use of a bulk mica substrate for graphene-based devices, however, hampers the ability to electrostatically doping graphene with a backgate. This limitation was overcome by employing 10–50 nm thick mica flakes deposited on SiO_2/Si substrates.[14] The 2D nature of these atomically thin crystalline insulator sheets makes them very interesting candidates in applications such as insulating barriers in planar tunnel junctions or as flexible substrates for graphene or molecular electronic devices. However, despite the large number of potential applications of these crystalline insulator nanosheets, the details about the fabrication, identification, and characterization of these ultrathin mica flakes are missing in the literature.

In this work the fabrication of atomically thin mica flakes as thin as just one layer thick (1 nm) on SiO_2/Si substrates is reported. Also presented is a combined characterization of these flakes by quantitative optical microscopy and atomic force microscopy (AFM). From this study, one can determine the optimal SiO_2 substrate thickness and illumination wavelength to reliably identify atomically thin crystals of mica by optical microscopy. In addition, an all-dry procedure to transfer few-layer graphene (FLG) flakes on top of atomically thin mica flakes is demonstrated, based on viscoelastic stamps like the ones used in soft lithography. From Raman spectroscopy measurements, it is concluded that this transfer technique produces cleaner and higher-quality flakes than conventional wet-transfer procedures based on lithographic resists.[8,15]

2. Results

2.1. Sample Fabrication

In order to produce atomically thin muscovite mica flakes, the micromechanical cleavage technique was employed, widely known from the fabrication of graphene flakes[2] and other materials.[16] To cleave the starting material, this technique usually employs an adhesive tape, which can leave traces of glue on the surface that contaminate the fabricated sample.[17] This problem can be avoided by replacing the adhesive tape by a viscoelastic stamp, similar to the ones used in soft-lithography.[18] In previous works, we successfully used stamps of poly(dimethyl)-siloxane (PDMS) to fabricate graphene,[19] $NbSe_2$, and MoS_2[3] atomically thin crystals. To produce atomically thin mica flakes, first a bulk muscovite mica sample is cleaved by pressing the surface of the stamp against the bulk mica and peeling it off suddenly. After this step of the process, part of the mica surface is cleaved and transferred to the stamp surface. Next, to transfer the mica flakes to an arbitrary surface, one presses the surface of the stamp against the receptor surface and peels it off slowly (5 s). Using this technique, mica flakes with thicknesses ranging from hundreds of nanometers down to just one nanometer have been produced, which is the thickness of a single layer of mica. While the chemical structure of mica is different from graphene (and so their chemical, electrical, and mechanical properties), the transfer rate and the area of atomically thin flakes is comparable to graphene prepared by mechanical exfoliation of highly oriented pyrolitic graphite (HOPG).

Figure 1a shows some mica flakes transferred onto a silicon substrate with a 300 nm SiO_2 capping layer. It was observed that the apparent color of a flake depends on its thickness. Figure 1b presents an optical micrograph under white illumination of a mica flake, with thickness ranging from 2 to 20 nm. The top insert in Figure 1b shows a contact-mode AFM topographic profile measured through the boundary between the SiO_2 surface and the mica flake. The

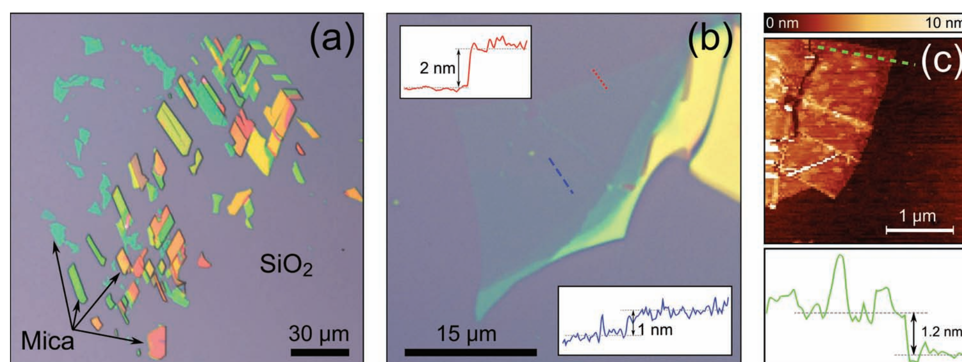

Figure 1. a) Optical micrograph of several mica flakes deposited on a 300 nm SiO_2/Si substrate by mechanical exfoliation. The different colors of the flakes correspond to different thicknesses. b) Optical micrograph of an ultrathin muscovite mica flake on a 300 nm SiO_2/Si substrate. Top insert in (b): contact-mode AFM topographic line profile measured across the interface between the mica flake and the SiO_2 substrate (dotted red line). The thickness of the flake in this region is 2 nm, which corresponds to the thickness of two single mica layers. Bottom insert in (b): the topographic profile (along the dashed blue line) showing the boundary between a region 2 nm thick and another 3 nm thick. c) Contact-mode AFM topographic image of a mica flake with a thickness of 1.2 nm, corresponding to a single layer of mica. A topographic profile along the green dashed line is shown below panel (c).

© 2011 Wiley-VCH Verlag GmbH & Co. KGaA, Weinheim

height difference between the SiO_2 substrate and the mica flake in this region is 2 nm, which corresponds to the thickness of two single layers of muscovite mica. The bottom insert in Figure 1b shows the contact-mode AFM topographic profile measured across the boundary between a region two layers thick and another three layers thick (3 nm thickness). Although it was found that single-layer flakes are usually not much larger than 1 μm × 1 μm (Figure 1c), the typical area of thin mica flakes (2 or 3 layers) can be up to 5 μm × 5 μm, but some of them can be significantly larger (Figure 1b). The large area of these nanometer-thick mica sheets, comparable to the one of exfoliated graphene flakes, makes them promising candidates for use not only as substrates for graphene-based devices but also as insulator barriers in planar tunnel junctions or as dielectrics in nanocapacitors.

2.2. Optical Characterization

The physics behind the optical visibility of these atomically thin crystals can be illustrated with the example of the interference colors in SiO_2 thin films. It is well known that the thickness of thermally grown SiO_2 layers on Si wafers can be readily determined with ≈5 nm accuracy from their color under white-light illumination.[20,21] This apparent color is due to the interference of the paths reflected at the air/SiO_2 and SiO_2/Si interfaces (similar to a Fabry–Perot interferometer). The interfering paths will have a relative phase shift, which depends on the illumination wavelength and the SiO_2 layer thickness, hence the SiO_2 thickness dependence of the color of the wafers. If one deposits a thin mica sheet instead of a SiO_2 layer the effect should be similar. If the mica sheet is atomically thin, the optical path difference could be small and the color difference between the mica sheet and the bare Si wafer could thus be imperceptible. The optical visibility of atomically thin crystals, however, can be enhanced by depositing them on a multilayered medium, typically a Si wafer with a thermally grown SiO_2 capping layer.[22]

To interpret the observed optical contrast one can employ a simple model based on the Fresnel law.[22,23] This approach has been successfully employed to study the optical contrast of different 2D crystals such as graphene,[22–24] transition metal dichalcogenides MoS_2 and $NbSe_2$,[3,25] or hexagonal boron nitride.[26] The subscripts 0, 1, 2, and 3 will label hereafter the air, mica flake, SiO_2, and Si media, respectively. Normal incidence of the light through the trilayer structure is considered formed by the mica flake, the SiO_2, and the Si. The optical properties of the Si layer, considered semi-infinite, are given by its complex refractive index $\tilde{n}_3(\lambda) = n_3 - i\kappa_3$, which strongly depends on the illumination wavelength (λ) in the visible range of the spectrum.[27] The SiO_2 layer, with a thickness d_2, is described by its refractive index $\tilde{n}_2(\lambda)$ which also depends on the illumination wavelength.[27] Note that, using the refractive indices of SiO_2 and Si, one can accurately account for the interference colors of the oxidized wafers with a Fresnel law-based model.[20,21] The reflected intensity for a SiO_2/Si wafer (I_0) can be expressed in terms of the phase shift produced by the SiO_2 layer ($\Phi_2 = 2\pi\tilde{n}_2 d_2/\lambda$) and the amplitudes of the paths reflected at the air/SiO_2 and SiO_2/Si interfaces (r_{02} and r_{23} respectively),

$$I_0(\lambda) = \left| \frac{r_{02} + r_{23} e^{-2i\Phi_2}}{1 + r_{02} r_{23} e^{-2i\Phi_2}} \right|^2 \tag{1}$$

where the amplitude of the reflected path in the interface between the media i and j is $r_{ij} = (\tilde{n}_i - \tilde{n}_j)/(\tilde{n}_i + \tilde{n}_j)$ with $\tilde{n}_j$ being the refractive index of medium j. The atomically thin mica crystal is taken into account as a layer of thickness d_1 on the SiO_2 medium, whose refractive index is $\tilde{n}_1(\lambda) = n_1 - i\kappa_1$. The reflected intensity from the mica flake (I_0) can be written as[22,23]

$$I_1(\lambda) = \left| \frac{r_{01} e^{i(\Phi_1+\Phi_2)} + r_{12} e^{-i(\Phi_1-\Phi_2)} + r_{23} e^{-i(\Phi_1+\Phi_2)} + r_{01} r_{12} r_{23} e^{i(\Phi_1-\Phi_2)}}{e^{i(\Phi_1+\Phi_2)} + r_{01} r_{12} e^{-i(\Phi_1-\Phi_2)} + r_{01} r_{23} e^{-i(\Phi_1+\Phi_2)} + r_{12} r_{23} e^{i(\Phi_1-\Phi_2)}} \right|^2 \tag{2}$$

$\Phi_1 = 2\pi\tilde{n}_1 d_1/\lambda$ is the phase shift of the path produced by the presence of the mica flake. Using the expressions (1) and (2), one can obtain the optical contrast (C) which is defined as

$$C = \frac{I_1 - I_0}{I_1 + I_0}. \tag{3}$$

Figure 2a shows the optical contrast, measured at different illumination wavelengths, for flakes 2–10 layers thick.

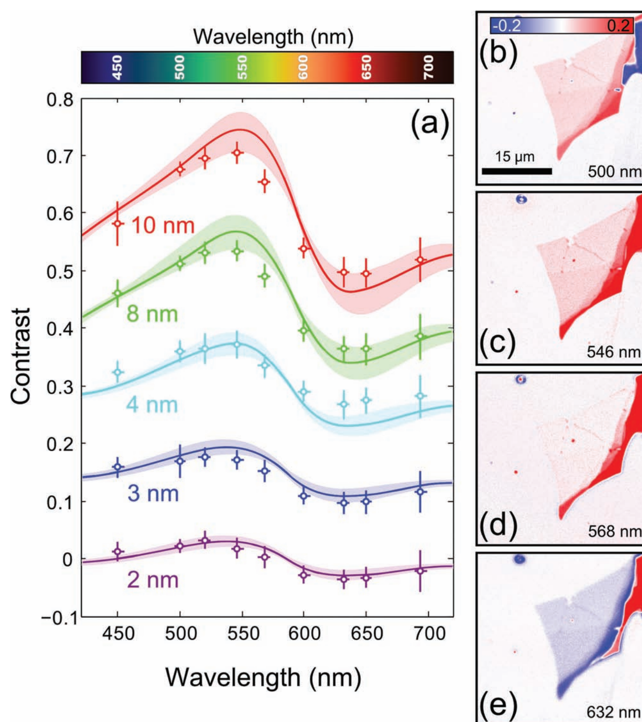

Figure 2. a) Optical contrast measured at different illumination wavelengths on mica flakes from 2 to 10 nm thick. The contrast-versus-wavelength dependence calculated with the Fresnel law-based model is also shown (solid lines). The refractive index of mica flakes is $n = 1.55$ ($\kappa = 0$) and an uncertainty in its value of $\Delta n \pm 0.1$ has been considered and is displayed as the grayed region enveloping the solid lines. Note that the data for the 3, 4, 8, and 10 nm have been vertically displaced for clarity by 0.15, 0.3, 0.45, and 0.6. b–e) Optical contrast maps measured, in the mica flake shown in Figure 1, at different illumination wavelengths.

© 2011 Wiley-VCH Verlag GmbH & Co. KGaA, Weinheim

The solid lines in the plot are the contrast versus wavelength dependencies according to expressions (1), (2), and (3). The thickness of the flake has been determined by contact-mode AFM and the refractive index of the mica flake is taken to be $\tilde{n}_1 = 1.55–0i$, that is independent from the illumination wavelength and similar to the one of bulk muscovite mica. The grayed areas enveloping the solid lines mark the calculated contrast versus wavelength dependencies considering an uncertainty of the real part of the refractive index $\Delta n_1 = \pm 0.1$. The measured optical contrast values are in good agreement with the calculated data indicating, within experimental resolution, that the refractive index of the atomically thin mica flakes can be considered close to its bulk value. Notice that in Figure 2a the experimental contrast is systematically slightly lower than the calculated one. This was observed in similar experiments[23] and was attributed to the finite numerical aperture of the microscope objective.[28] Figure 2b shows the optical contrast maps for the same mica flake shown in Figure 1b at 500, 546, 568, and 632 nm illumination wavelengths. In agreement with the data shown in Figure 2a, at $\lambda = 568$ nm the optical contrast of the thinnest part of the flake vanishes while it shows a maximum (minimum) at $\lambda = 520$ (630) nm.

Expressions (1), (2), and (3), can also be used to calculate the optical contrast yielded by a single layer of mica for different illumination wavelengths and SiO_2 capping-layer thicknesses. **Figure 3** shows the result of this calculation, which can be used as a guide to find the appropriate conditions to identify ultrathin mica flakes atop SiO_2/Si substrates. SiO_2 thicknesses were selected that optimize the contrast for $\lambda = 550$ nm, which is the illumination wavelength to which the human eye attains maximum sensitivity.[29] The first four different SiO_2 thicknesses which optimize the optical contrast for a single layer of mica are: 55 nm (–1.5% contrast, nearly λ-independent), 100 nm (+1.5% contrast, also nearly λ-independent), 260 nm (–1.5% at $\lambda = 550$ nm and 0% at $\lambda = 500$ nm) and 305 nm (+1.5% at $\lambda = 550$ nm and 0% at $\lambda = 580$ nm). Note that 1.5% contrast is roughly the detection limit of the human eye and thus special care has to be taken to optimize both illumination wavelength and SiO_2 thickness in order to identify these ultrathin mica flakes by eye. The source of such a low optical contrast is that the absorption of mica in the visible spectrum is very low and thus the optical contrast is mainly due to the optical path difference due to the presence of the atomically thin mica flake. On the contrary, Roddaro et al.[22] reported that the opacity of graphene is the key element to explain the optical contrast of graphene layers and the interference color only plays a marginal role in the visibility.

It is common practice to assist the optical characterization of layered materials with their Raman spectra. Such spectra turned out to be especially informative in the case of graphene, where the precise distinction between single, double, and multilayer samples is possible.[30,31] We measured the Raman spectrum for the mica flakes of different thicknesses, ranging from 2 nm (2 layers) to 10 nm (10 layers) deposited on 300 nm SiO_2 and for bulk mica. None of the spectra of thin mica flakes showed typical Raman bands of bulk mica, even after long acquisition times (5 min), presenting only the spectral features of its substrate: silicon (a strong Lorentzian peak at ≈520 cm^{-1}) and a broad flat band between 930 and 1000 cm^{-1} (see **Figure 4**a). For comparison,

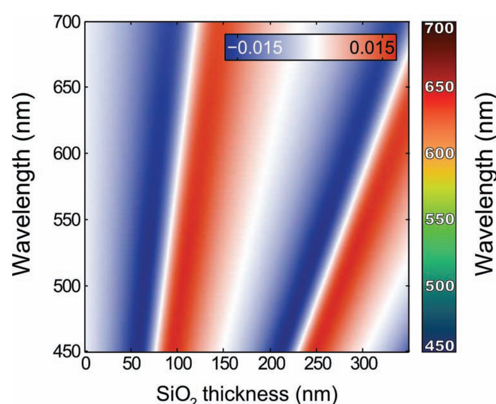

Figure 3. Color map of the calculated optical contrast for a monolayer mica flake as a function of the illumination wavelength and the SiO_2 thickness. The color bar inserted in the plot shows the opitcal contrast while the one at the right indicates the color of the illumination light.

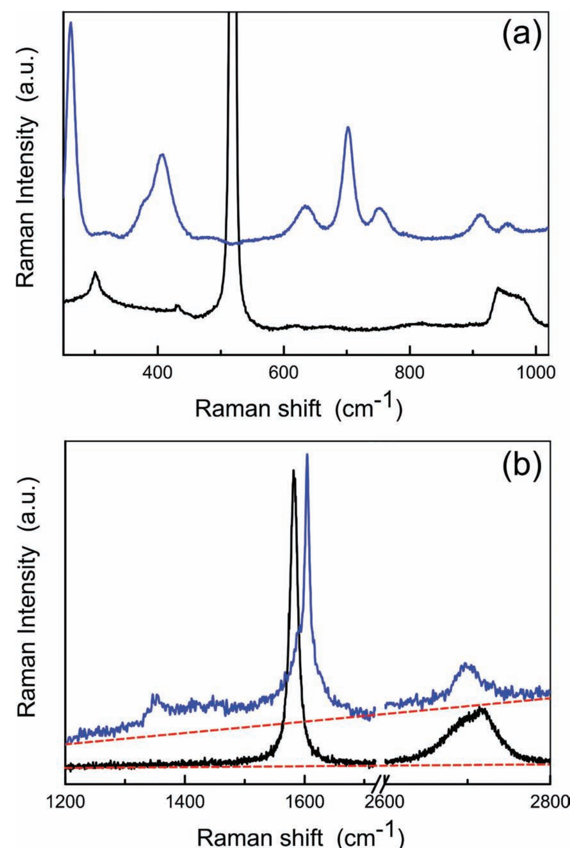

Figure 4. a) Raman spectra of a thin mica flake (less than 12 nm thick) on SiO_2/Si (black) and bulk mica (blue), a parent material for analyzed flakes. For mica flakes from 2 to 60 nm thick, Raman spectra showed only features of the Si underneath. No peaks corresponding to mica vibrational modes can be resolved. b) Raman spectrum of multilayer graphene after PDMS-based transfer (black) and the spectrum of single layer graphene after poly(methyl methacrylate) (PMMA)-based transfer (blue). No baseline corrections were applied to the spectra. The strong linear increase of the background, emphasized by a red dashed line as an eye-guide, for the case of PMMA-based transfer is apparent.

© 2011 Wiley-VCH Verlag GmbH & Co. KGaA, Weinheim

small NANO MICRO

we also measured Raman spectra of the parent material, bulk mica, containing all typical Raman bands known from the literature (**Figure 5**b).[32] From this we conclude that the thin mica flakes give too weak a signal to be detected in Raman, excluding Raman spectroscopy as a useful tool for its detection and investigation. Invisibility of the mica flakes in Raman spectra, however, carries a large advantage because it means that spectra won't interfere with the Raman signature of materials deposited on top. Such an interference of Raman signatures occurs in the case of graphene, when deposited on hexagonal boron nitride (BN), which was proposed as an advantageous new substrate for graphene electronics due to its surface that is flat and free from trapped charges.[8] In BN, a main vibrational Raman mode (E2g) occurs at ≈1366 cm^{-1} and its large intensity can screen in the spectrum the D-band of graphene (which occurs at 1344 cm^{-1} and as induced by defects gives a valuable information about the flake quality). From this point of view, the invisibility of the thin mica flakes in Raman ensures the proper detection of all graphene Raman bands when deposited on top.

2.3. Transfer of FLG on Top of Thin Mica Flakes

As pointed out in the introduction, ultrathin mica flakes can be very appealing substrates to fabricate graphene electronic devices. By depositing graphene on top of an ultrathin mica flake one can uncouple the graphene flake from the SiO_2 substrate while maintaining the possibility of applying an electric field through the SiO_2/mica to change the graphene doping. In this work we present an all-dry procedure to transfer few-layer graphene (FLG) flakes on top of thin mica flakes.

The main steps of the procedure are depicted in Figure 5a. First, a PDMS stamp is used to cleave an HOPG graphite sample. Second, FLG flakes are identified on the PDMS surface by optical inspection in transmission-mode optical microscopy. Third, because the PDMS stamp is transparent, the selected FLG flake can be accurately aligned to the target mica flake, using a 3-axis micropositioner stage attached to an optical microscope, which has been previously deposited onto a 300 nm SiO_2/Si substrate. Fourth, the PDMS stamp is brought into contact with the substrate and subsequently peeled off very slowly (5 s). In this way, the FLG flake is transferred on top of the mica flake. Figure 5b shows an optical microscopy image of a 10 layer-thick graphene flake deposited on top of a 12 layer-thick mica flake. Additionally, we inspect the graphene flake using Raman spectroscopy. As Raman measurements are sensitive to fluorescent background, they give information not only about the quality of the transferred flake but also about the organic/polymer traces left after the transfer process. In Figure 4 we compare the Raman spectra of the flake transferred to SiO_2 with PDMS stamps and the flake transferred with a wet-transfer technique based on poly(methyl methacrylate) (PMMA) resist.[8,15] The acquisition conditions were the same for both samples, with the same setup used to study the mica flake. The flakes transferred with PDMS stamps only show a small constant background, which can be attributed to thermal fluctuations of the CCD detector. The flake also does not exhibit defects (no D-band at 1344 cm^{-1}) and well resemble spectra of the freshly cleaved, pristine few layer graphene. On the contrary, the flake obtained by transferring with PMMA shows small D-band (5% of the G-band intensity), indicating some lattice defects or adsorbates and a much larger linearly increasing background, which is a signature of fluorescent contaminants. The ratio between G-band (≈1580 cm^{-1}) and 2D-band (≈2680 cm^{-1}) is below 1, indicating high doping of the flake. We have additionally found that all the Raman signatures of the few layers graphene flake transferred on top of the thin mica flake remains unmodified, proving the convenience of ultrathin mica flakes in applications that require atomically flat substrates that are inactive to Raman spectroscopy. From that, one can conclude that this all-dry transfer technique yields flakes of much higher quality, which are desirable for making the most of its remarkable electronic properties.

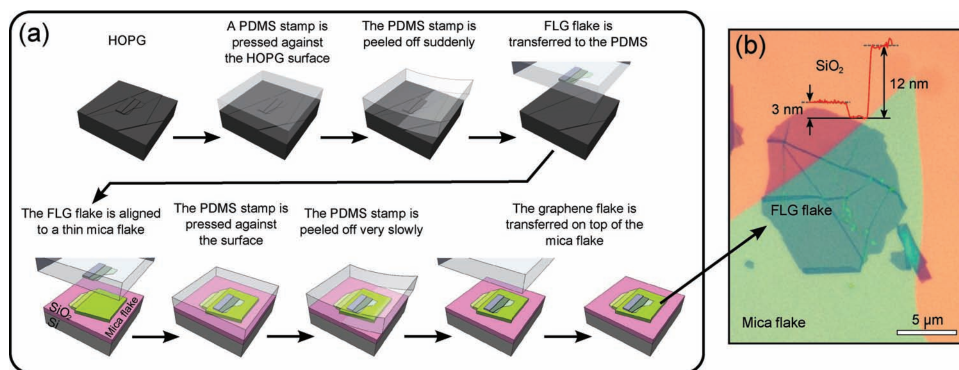

Figure 5. a) Schematic diagram of the transfer procedure to deposit FLG flakes on top of a thin mica flake. We first cleave a bulk HOPG sample with a PDMS stamp. Then the stamp is inspected with an optical microscope in transmission mode to find thin graphite flakes. The selected flake is aligned to a thin mica flake previously deposited on a 300 nm SiO_2/Si substrate by micromechanical cleavage. The stamp is brought into contact with the surface and it is peeled off very slowly. The FLG flake is then transferred on top of the mica flake. b) Optical micrograph of a 3 nm thick FLG on top of a 12 nm thick mica flake. The AFM topographic profile measured along the solid black line is also shown in the image.

 © 2011 Wiley-VCH Verlag GmbH & Co. KGaA, Weinheim

3. Conclusion

We have deposited atomically thin mica flakes on SiO_2/Si wafers using a procedure based on mechanical exfoliation with viscoelastic PDMS stamps. This procedure yields mica crystals whose thickness can be as small as that of a single layer. We have studied the optical contrast of flakes with thicknesses ranging from 2 to 10 nm, measured at different illumination wavelengths. We find that the measured optical contrast can be accurately accounted for by a model based on the Fresnel law. Using this model we have determined the optimal silicon oxide thickness and illumination wavelength to reliably identify, by optical microscopy, atomically thin mica flakes deposited on SiO_2/Si substrates. In addition, we have developed an all-dry procedure to transfer few-layer graphene flakes on top of atomically thin mica flakes, using again viscoelastic stamps. Raman spectra measurements have been used to characterize the quality of the transferred flake and also to get information about the organic/polymer traces left after the transfer process. We have found that our transfer technique produces cleaner and higher quality flakes than conventional wet-transfer procedures based on lithographic resist such as PMMA. The experimental realization of these crystalline atomically thin insulating sheets expands an interesting family of 2D crystals. Moreover, the combination of these mica sheets with other materials such as graphene or MoS_2 can be used to engineer atomically thin crystalline heterostructures.

4. Experimental Section

The poly(dimethyl)-siloxane (PDMS) stamps, used during the mica flake preparation and the all-dry transfer procedure, have been cast by curing the Sylgard 184 elastomer kit purchased from Dow Corning.[3]

The atomic force microscope (AFM) used for the thickness measurement of the flakes is a Nanotec Cervantes AFM (Nanotec Electronica) operated in contact mode under ambient conditions. We have selected contact-mode AFM instead of dynamic modes of operation to avoid artifacts in the determination of flake thickness.[33]

The quantitative measurements of the optical contrast of ultrathin mica flakes has been done with a Nikon Eclipse LV100 optical microscope under normal incidence with a 50× objective (numerical aperture NA = 0.8) and with a digital camera EO-1918C 1/1.8″ (from Edmund Optics) attached to the microscope trinocular. The illumination wavelength was selected by means of nine narrow band-pass filters (10 nm FWHM) with central wavelengths 450, 500, 520, 546, 568, 600, 632, 650 and 694 nm purchased from Edmund Optics.

The Raman spectra were recorded at room temperature using Horiba T64000 Raman spectrometer with 532 nm laser excitation wavelength of unpolarized light (resolution ≈2 cm^{-1}). The spot size was <10 µm in diameter and the power density was about 30 W cm^{-2}.

Acknowledgements

A.C-G. acknowledges fellowship support from the Comunidad de Madrid (Spain) and also the Universidad Autónoma de Madrid (Spain) for the mobility grant to work in Physics of Nanodevices Group (University of Groningen, Netherlands). This work was supported by MICINN (Spain) (MAT2008-01735 and CONSOLIDER en Nanociencia molecular CSD-2007-00010). M.W. is grateful to Optical Condensed Matter Group at University of Groningen (Netherlands) and especially to Ben Hesp for the access to Raman facilities and help with measurements. M.W. and N.T. acknowledge financial support from Ubbo Emmius program of Groningen Graduate School of Science and Zernike Institute for Advanced Materials, respectively.

[1] K. Novoselov, D. Jiang, F. Schedin, T. Booth, V. Khotkevich, S. Morozov, A. Geim, *Proc. Natl. Acad. Sci. USA* **2005**, *102*, 10451.
[2] K. S. Novoselov, A. K. Geim, S. V. Morozov, D. Jiang, Y. Zhang, S. V. Dubonos, I. V. Grigorieva, A. A. Firsov, *Science* **2004**, *306*, 666.
[3] A. Castellanos-Gomez, N. Agrait, G. Rubio-Bollinger, *Appl. Phys. Lett.* **2010**, *96*, 213116.
[4] C. Lee, H. Yan, L. E. Brus, T. F. Heinz, J. Hone, S. Ryu, *ACS Nano* **2010**, *4*, 2695.
[5] H. S. S. Ramakrishna Matte, A. Gomathi, A. K. Manna, D. J. Late, R. Datta, S. K. Pati, C. N. R. Rao, *Angew. Chem.* **2010**, *122*, 4153.
[6] A. Splendiani, L. Sun, Y. Zhang, T. Li, J. Kim, C.-Y. Chim, G. Galli, F. Wang, *Nano Lett.* **2010**.
[7] D. Pacile, J. Meyer, Ç. Girit, A. Zettl, *Appl. Phys. Lett.* **2008**, *92*, 133107.
[8] C. Dean, A. Young, I. Meric, C. Lee, L. Wang, S. Sorgenfrei, K. Watanabe, T. Taniguchi, P. Kim, K. Shepard, *Nature Nanotechnol.* **2010**, *5*, 722.
[9] C. Lui, L. Liu, K. Mak, G. Flynn, T. Heinz, *Nature* **2009**, *462*, 339.
[10] V. Geringer, M. Liebmann, T. Echtermeyer, S. Runte, M. Schmidt, R. Rückamp, M. C. Lemme, M. Morgenstern, *Phys. Rev. Lett.* **2009**, *102*, 076102/1.
[11] J. C. Meyer, A. K. Geim, M. I. Katsnelson, K. S. Novoselov, T. J. Booth, S. Roth, *Nature* **2007**, *446*, 60.
[12] M. L. Teague, A. P. Lai, J. Velasco, C. R. Hughes, A. D. Beyer, M. W. Bockrath, C. N. Lau, N. C. Yeh, *Nano Lett.* **2009**, *9*, 2542.
[13] A. Castellanos-Gomez, R. H. Smit, N. Agrait, G. Rubio-Bollinger, unpublished.
[14] L. Ponomarenko, R. Yang, T. Mohiuddin, M. Katsnelson, K. Novoselov, S. Morozov, A. Zhukov, F. Schedin, E. Hill, A. Geim, *Phys. Rev. Lett.* **2009**, *102*, 206603.
[15] A. Reina, X. Jia, J. Ho, D. Nezich, H. Son, V. Bulovic, M. Dresselhaus, J. Kong, *Nano Lett.* **2008**, *9*, 30.
[16] K. Kalantar-zadeh, J. Tang, M. Wang, K. L. Wang, A. Shailos, K. Galatsis, R. Kojima, V. Strong, A. Lech, W. Wlodarski, R. B. Kaner, *Nanoscale* **2010**, *2*, 429.
[17] J. Moser, A. Verdaguer, D. Jiménez, A. Barreiro, A. Bachtold, *Appl. Phys. Lett.* **2009**, *92*, 123507.
[18] M. A. Meitl, Z. T. Zhu, V. Kumar, K. J. Lee, X. Feng, Y. Y. Huang, I. Adesida, R. G. Nuzzo, J. A. Rogers, *Nat. Mater.* **2006**, *5*, 33.
[19] M. Moreno-Moreno, A. Castellanos-Gomez, G. Rubio-Bollinger, J. Gomez-Herrero, N. Agraït, *Small* **2009**, *5*, 924.

© 2011 Wiley-VCH Verlag GmbH & Co. KGaA, Weinheim

[20] J. Kvavle, C. Bell, J. Henrie, S. Schultz, A. Hawkins, *Opt. Express* **2004**, *12*, 5789.
[21] J. Henrie, S. Kellis, S. Schultz, A. Hawkins, *Opt. Express* **2004**, *12*, 1464.
[22] S. Roddaro, P. Pingue, V. Piazza, V. Pellegrini, F. Beltram, *Nano Lett.* **2007**, *7*, 2707.
[23] P. Blake, E. W. Hill, A. H. C. Neto, K. S. Novoselov, D. Jiang, R. Yang, T. J. Booth, A. K. Geim, *Appl. Phys. Lett.* **2007**, *91*, 063124.
[24] I. Jung, M. Pelton, R. Piner, D. Dikin, S. Stankovich, S. Watcharotone, M. Hausner, R. Ruoff, *Nano Lett.* **2007**, *7*, 3569.
[25] M. Benameur, B. Radisavljevic, J. Héron, S. Sahoo, H. Berger, A. Kis, *Nanotechnology* **2011**, *22*, 125706.
[26] R. V. Gorbachev, I. Riaz, R. R. Nair, R. Jalil, L. Britnell, B. D. Belle, E. W. Hill, K. S. Novoselov, K. Watanabe, T. Taniguchi, A. K. Geim, P. Blake, *Small* **2011**, *7*, 465.
[27] C. Herzinger, B. Johs, W. McGahan, J. Woollam, W. Paulson, *J. Appl. Phys.* **1998**, *83*, 3323.
[28] C. Casiraghi, A. Hartschuh, E. Lidorikis, H. Qian, H. Harutyunyan, T. Gokus, K. Novoselov, A. Ferrari, *Nano Lett.* **2007**, *7*, 2711.
[29] G. Wald, *Science* **1945**, *101*, 653.
[30] D. Graf, F. Molitor, K. Ensslin, C. Stampfer, A. Jungen, C. Hierold, L. Wirtz, *Nano Lett.* **2007**, *7*, 238.
[31] D. Graf, F. Molitor, K. Ensslin, C. Stampfer, A. Jungen, C. Hierold, L. Wirtz, *Solid State Commun.* **2007**, *143*, 44.
[32] D. McKeown, M. Bell, E. Etz, *Am. Mineral.* **1999**, *84*, 1041.
[33] P. Nemes-Incze, Z. Osváth, K. Kamarás, L. P. Biró, *Carbon* **2008**, *46*, 1435.

Received: April 15, 2011
Published online: August 1, 2011

© 2011 Wiley-VCH Verlag GmbH & Co. KGaA, Weinheim